

Heterogeneous solution reactions between MBr_3 ($\text{M} = \text{Ga}, \text{In}$) and Li_3N . Formation and characterization of nanocrystalline GaN powders

R. L. WELLS and J. F. JANIK*

Department of Chemistry, Paul M. Gross Chemical Laboratory,
Duke University, Durham, NC 27708-0346, U.S.A.

* On leave from: University of Mining and Metallurgy, Krakow, Poland

(H. W. R., received July 1, 1996 ; accepted August 27, 1996.)

ABSTRACT. - Heterogeneous reactions between MBr_3 ($\text{M} = \text{Ga}, \text{In}$) and Li_3N in refluxing aromatic or aromatic/diglyme solvents were investigated as a potential route to nanocrystalline GaN and InN powders. For $\text{M} = \text{Ga}$, the pyrolysis of the as-prepared precursors at 450-500 °C under vacuum or NH_3 yielded nanosized GaN and elemental Ga. Gallium nitride was characterized by XRD, XPS and UV/vis spectroscopies, TEM microscopy, and elemental analysis. For $\text{M} = \text{In}$, the reactions were highly solvent dependent and resulted exclusively in redox products such as indium(I) bromide, InBr, and elemental In.

INTRODUCTION

Gallium nitride, GaN, is a broad band semiconducting material with great potential for optoelectronic applications in the blue and UV spectral range [1]. Its most common hexagonal form has a direct band gap of 3.4 eV. Indium nitride, InN, is a narrow band semiconductor with a band gap of 1.9 eV, which predestines it to combinations with GaN since the hexagonal varieties of both nitrides form solid

solutions with continuous band gap ranging from 1.9 eV to 3.4 eV [2]. The vast majority of studies on GaN and InN has been concerned with thin nitride films as prototype electronic devices formed by a variety of deposition techniques [1,3]. Relatively fewer reports are available on the preparation and characterization of the bulk nitrides [4].

One approach to the synthesis of Group 13 - Group 15 binary and ternary compounds involves a modification of self-propagating high-temperature synthesis or solid state metathesis reactions between alkaline metal pnictides and Group 13 halides [5]. Such reactions [6] and their modifications using lithium amides [7] or sodium azide [8] have also been applied to the preparation of binary and ternary transition metal and lanthanide pnictides. Particularly, some binary and ternary transition metal nitrides have been prepared by combination of Li_3N and metal halides [5g,6d-f]. However, there have been only a few reports on the synthesis of Group 13 nitrides by the above methods, e.i. BN [5c] and AlN [5d].

A successful modification of the metathetical reaction carried out in organic solvents was developed in our laboratory for the synthesis of the nanocrystalline 13-15 semiconductors GaP, GaAs, InP, InAs, and InSb [9]. In this regard, glyme solvents were found to be particularly useful in producing reduced sizes of nanocrystalline particles of GaAs and GaP. The presence of the relatively strong coordinating ether in the system was thought to be advantageous for two major reasons. First, the multidentate glyme ethers have been known to form ionic coordinated complexes with aluminum and gallium halides [10], a property that could facilitate the metathetical reaction. Second, such solvents might influence a crystallite growth rate by capping surface active sites. This method as well as a parallel, equally effective dehalosilylation route [11] have enabled us to prepare a growing number of 13-15 nanosized materials.

Many physical properties of the semiconductors are size-dependent [12]. For example, the quantum confinement effect has been demonstrated for particle sizes smaller than an excitonic Bohr radius of a given compound where distinct electronic levels exist with energies higher than the band gap of the bulk material (blue shift). For 13-15 semiconductors, few reports are available on the synthesis of nanocrystalline materials and their optical properties in this size regime [5f,9,11,13].

Described herein is a study on the independent metathetical reactions of GaBr_3 and InBr_3 with Li_3N in aromatic or aromatic/diglyme solvents. The specific choice of bromides was dictated by the fact that the ether soluble LiBr by-product could easily be removed from the system.

EXPERIMENTAL SECTION

General techniques. All the manipulations were performed in an argon filled Vacuum Atmospheres Dry-Lab He-493 or using standard vacuum/Schlenk techniques [14]. Solvents were dried over and distilled from Na benzophenyl ketyl prior to use. Anhydrous $GaBr_3$ (99.999 %), $InBr_3$ (99.999 %), and Li_3N (99.5 %) were purchased from Strem Chemicals and used as received (both $GaBr_3$ and $InBr_3$ were stated to be of 99.5% purity with residual oxide contaminant; the nitrogen assay in Li_3N was quoted to be in the 37-38 % range (theoretical: 40.2 %) and the remaining lithium mainly bound as oxide). Anhydrous NH_3 was obtained from Matheson Gas Products and in pyrolysis studies was used as received. XRD data were collected for oil coated samples on a Phillips XRD 3000 diffractometer using $Cu K\alpha$ radiation. XPS analyses were obtained at the XPS facility of the University of North Carolina at Chapel Hill with data collected on a Perkin-Elmer PH1 5400 system using $Mg K\alpha$ and 3 KeV argon sputtering. HRTEM microscopy was performed on a Topcon EM002B instrument using 200 KV accelerating voltage at the Analytical Instrumental Facility of North Carolina State University. UV/vis absorption spectra were obtained for methanol suspensions vs. blank methanol between 190 and 820 nm on a Hewlett-Packard 8452A diode array spectrophotometer. IR spectra were acquired for KBr pellets on a BOMEM Michelson MB-100 FT-IR spectrometer.

Reactions between $GaBr_3$ and Li_3N .

Caution: one should avoid a direct mixing of the solid $GaBr_3$ and Li_3N without solvent because they were found to exothermically self-ignite upon contact.

(a) Reaction in xylene/diglyme. In the dry box, 0.940 g of $GaBr_3$ (3.05 mmol) was placed in a 300 mL flask together with 70 mL of xylene and 70 mL of diglyme. To this mixture, 0.104 g of Li_3N (3.00 mmol) was added resulting in a dark brown/red slurry. The mixture was refluxed under argon for 80 h. Upon completion of reflux, the supernatant was removed, the solid was washed three times with 50 mL of Et_2O to remove $LiBr$, and evacuated overnight. The product was heated in a sublimator at 450 °C under vacuum for 20 h. Some metallic droplets, assumed to be elemental gallium, condensed on the cold finger and the main product was recovered as a light gray powdery solid. The XRD spectrum of the latter displayed two broad features centered at approx. 2θ 35° and 60° and the IR spectrum showed a strong, broad band at 620 cm^{-1} and a weak band at 3400 cm^{-1} . The powder formed a well dispersed colloidal solution in methanol for which a UV/vis

absorption spectrum was obtained (absorption edge at 290 nm). The above reaction was also performed in refluxing diglyme. In this case, the as-prepared light gray precursor was heated in the sublimator at 200 °C under vacuum. Only minute quantities of metallic Ga were found on the cold finger. The XRD spectrum for the product showed two broad bands centered at 2θ 35° and 60°.

(b) Reaction in xylene. In the dry box, 0.940 g of GaBr₃ (3.05 mmol) was dissolved in 150 mL of xylene in a 300 mL flask equipped with a water condenser and 0.104 g of Li₃N (3.00 mmol) was added. Refluxing the mixture under argon for 80 h resulted in a gray slurry. The supernatant was removed, the solid washed three times with 50 mL of Et₂O to remove LiBr, and evacuated overnight to afford a gray powdery solid. The reaction was also performed in mesitylene and, in which case, a darker product was obtained. A UV/vis spectrum was obtained for a settled clear MeOH solution of the solid (absorption edge at 310 nm). The as-prepared solid was heated in a sublimator at 450 °C under vacuum overnight yielding a dark gray product and small quantities of metallic droplets condensed on the cold finger. The XRD spectrum showed broad but resolved bands that were indexed as hexagonal GaN. The XPS experiment for the solid showed relatively low nitrogen contents that further diminished with sputtering time. The curve fitting analysis of Ga binding energies also suggested the presence of metallic Ga and Ga-O species. No lithium or bromine was detected. Elemental analysis: calcd for GaN(%): Ga, 83.27; N, 16.73; found(%): Ga, 65.96; N, 3.49. Based on nitrogen, this amounted to 20.8 % GaN content. In one run, the solid obtained at 450 °C under vacuum was further pyrolyzed at 500 °C under a flow of NH₃ overnight. The XRD spectrum for the product showed the resolved peaks for hexagonal GaN. Anal. Calcd for GaN(%): Ga, 83.27; N, 16.73. Found(%): Ga, 71.76; N, 8.88; C, 2.47 or, based on nitrogen, 53% GaN content. For a series of the clear MeOH suspensions from different runs, a distinct peak feature was observed with an absorption edge between 290 and 310 nm. HRTEM microscopy was used for both the settled coarse particles and fine particles obtained from the evacuated clear solution. In both cases, a polycrystalline material was observed. A selected area electron diffraction pattern for the coarse solid showed numerous spots superimposed on diffuse rings that were indexed as hexagonal GaN. An electron diffraction pattern for the fine particles consisted of mostly diffuse rings with sparse spots indicating nanocrystalline GaN. The observed lattice fringes were identified as (0002) planes of hexagonal GaN.

Reactions between $InBr_3$ and Li_3N . The reactions in this system were performed in a similar fashion as described for GaN . However due to the reported instability of InN [15], all pyrolysis experiments were carried out at 250-300 °C under nitrogen atmosphere. For the reaction in xylene/diglyme, the final pyrolyzed product was shown by XRD to be a mixture of elemental In and In_2O_3 . Similarly, for the reaction in xylene, the resulting pyrolyzed product consisted of a mixture of indium(I) bromide, $InBr$, and elemental In . The latter results were fully corroborated by XPS measurements. The XPS data for the product were consistent with the presence of mostly indium(I) bromide species and elemental In . Small quantities of In_2O_3 were also observed. The deconvolution of the carbon and oxygen signals was consistent with the presence of an oxidized form of carbon in addition to its adventitious form, which supported the origin of the former from ether cleavage. No lithium was detected.

RESULTS AND DISCUSSION

The reaction of $GaBr_3$ with Li_3N occurred spontaneously upon mixing the two solids as a self-igniting, highly exothermic, and uncontrollable process similar to the reported solid state metathesis reactions in related systems [5]. However, the reactions between $GaBr_3$ and Li_3N could safely be performed in diglyme, aromatic/diglyme, and aromatic (xylene, mesitylene) solvents yielding, after the removal of $LiBr$ with Et_2O , light gray to dark gray precursors that were converted to nanocrystalline GaN and elemental Ga upon heating at 450 °C under vacuum. The additional pyrolysis at 500 °C under the flow of NH_3 improved the purity of the final GaN product. The ammonia treatment was thought to remove any end-site residual bromine atoms through ammonolysis with subsequent formation of sublimable NH_4Br and, simultaneously, preserve the GaN nanocrystalline habit.

Based on nitrogen analysis, a GaN content of 53 % was obtained from the pyrolysis at 500 °C under NH_3 . This could not be confirmed in a parallel manner by XPS spectroscopy because the method was found to yield unreliable nitrogen estimations due to preferential nitrogen sputtering from such materials [3e,16]. In order to see these results in a proper context, one has to be aware of the quite frequent failure of conventional elemental analysis when applied to both the 13-15 precursors and resulting solid state materials [6d,7,17]. For example, an elaborate method taking into account a refractory nature of the metal nitrides and their resistance to

oxidation at high temperatures had to be designed to improve the nitrogen analysis in VN by the factor of 2 compared with conventional combustion analysis [6d].

The crystallinity of the final product was dependent on both the solvent medium used for metathesis and the pyrolysis temperature. Figure 1 shows the XRD diffractograms obtained for two various products. Two unresolved, broad features

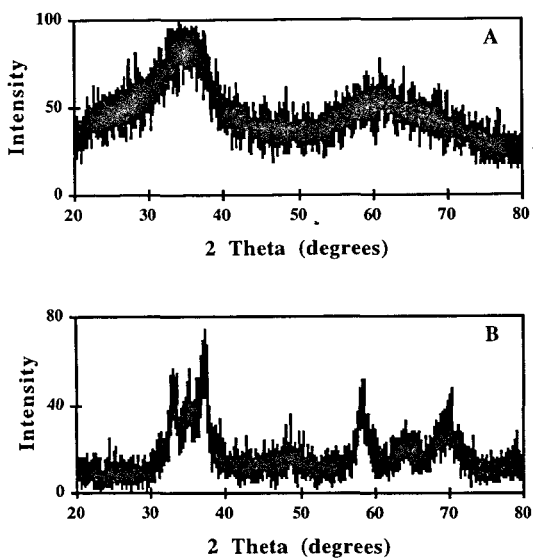


Fig.1 - XRD spectra of nanocrystalline GaN. (A) Product from reaction in xylene/diglyme; heated at 450 °C under vacuum. (B) Product from reaction in xylene; heated at 500 °C under NH₃ atmosphere.

at 2θ 35° and 60° were observed for the material from the reaction in xylene/diglyme and heating at 450 °C under vacuum (Fig.1A). An almost identical spectrum was obtained for the material from the reaction in diglyme which was later heated at 200 °C under vacuum. The products from the reactions in exclusively aromatic solvents followed by the pyrolysis at 450 °C under vacuum showed broad but partially resolved peaks, which were indexed as hexagonal GaN (Fig.1B). The two unresolved, broad XRD peaks in Fig.1A were in the region of the strong diffraction peak clusters for hexagonal GaN and could indicate the onset of the crystallinity of GaN [4a,4c]. The Scherrer estimation applied to peaks in Fig.1B gave the average particle size of 5 nm.

It was clear that the application of diglyme had a pronounced effect on the size of the particles. The onset of nanosized crystallinity was already observed for the solid from the reaction in diglyme, which was later heated at a temperature as low as 200 °C. At the same time, the solid from the reaction in xylene, which was subsequently heated at 450 °C, showed similar and rather low degree of crystallinity (Fig.1A). This had to be compared with the solid from the reaction in exclusively xylene that also was heated at 450 °C (Fig.1B), and which was estimated to contain larger crystallites. However, a side effect of the glyme capping behavior would manifest itself in a thermally induced ether cleavage and retention of surface oxygen in the solid nanoparticles.

In order to stabilize and characterize the nanocrystalline GaN particles, methanol suspensions of the products were prepared. The formation of the MeOH stabilized particles of GaAs, GaP, and others in colloidal solutions has already been explored in our laboratory and described elsewhere [9a,e,f]. The typical results of the UV/vis determinations for the GaN methanol suspensions are shown in Figure 2. Spectrum A was obtained for the as-prepared solid in refluxing xylene. It contained a shoulder feature with absorption edge at 310 nm. For the solid heated at 450 °C and treated

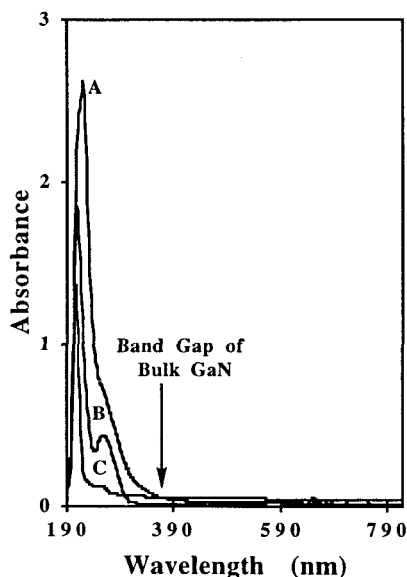


Fig. 2 - UV/vis spectra of methanol suspensions of nanocrystalline GaN. (A) As-prepared product from reaction in xylene. (B) Product from reaction in xylene; heated at 450 °C under vacuum. (C) Product from reaction in xylene/diglyme; heated at 450 °C under vacuum.

with MeOH, the UV/vis spectrum showed a distinct peak feature with absorption edge at 305 nm (spectrum B). Spectrum C was determined for the product from the reaction in xylene/diglyme heated at 450 °C. Generally, the absorption spectra obtained for a series of samples provided with the values for absorption edge in the range from 290 to 310 nm (4.28 to 4.00 eV). This has to be compared with the value of 366 nm (3.4 eV at 300 K) for the absorption edge of bulk GaN. If one assumed that the shoulder and peak features were due to the nanosized GaN particles, this represented a blue shift of the GaN absorption edge ranging from 0.60 to 0.88 eV. Based on these values, a particle size responsible for a given shift was obtained from equation 1 [12b,c]:

$$E = E_g + \frac{\hbar^2 \pi^2}{2R^2} \left[\frac{1}{m_e^* m_e} + \frac{1}{m_h^* m_e} \right] - \frac{1.8e^2}{4\pi\epsilon_r\epsilon_0 R} \quad (1)$$

where E is the energy of the observed absorption edge, E_g is 3.4 eV, m_e^* (0.20) and m_h^* (0.80) are the effective masses of the electron and the hole in GaN, respectively, m_e is the electron rest mass, e is the fundamental charge, ϵ_r is the dielectric constant for bulk GaN (9.0), ϵ_0 is the permittivity of vacuum, and R is the particle radius. For the range of the observed shifts, i.e. from 3.4 eV to 4.00 eV and 4.28 eV, the corresponding R values were calculated at 1.75 nm and 1.48 nm, respectively, or 3.5 to 3.0 nm diameters. These values were in a reasonable agreement with the particle size derived from the XRD spectra, especially when one realized that the XRD data were obtained for the bulk, but the UV/vis data were acquired for the smallest crystallite fraction in the MeOH solution. Some examples of the studies reporting excitonic transitions in semiconductors include investigations of GaAs [9a,d,13d,e,18], CdS [19], CdSe [12c,20], InP [13f], and InP, GaP, and GaInP₂ [13b]. However, at least in one case, the observed feature in the UV/vis spectrum for nanocrystalline GaAs was subject to a critical evaluation. It was suggested that this feature is caused by some unidentified molecular species rather than by the nanocrystalline GaAs particles [18a,b]. In our judgment, our interpretation of the UV/vis spectra is coherent and consistent with the assignment of the absorption feature to the excitonic absorption by the GaN nanoparticles.

TEM microscopy provided very strong evidence for the nanocrystalline GaN particles both in the bulk solid and the solid obtained from the clear, settled colloidal MeOH solution after removal of volatiles. Figure 3 shows the typical images obtained in this study. For the bulk solid, they mostly consisted of polycrystalline

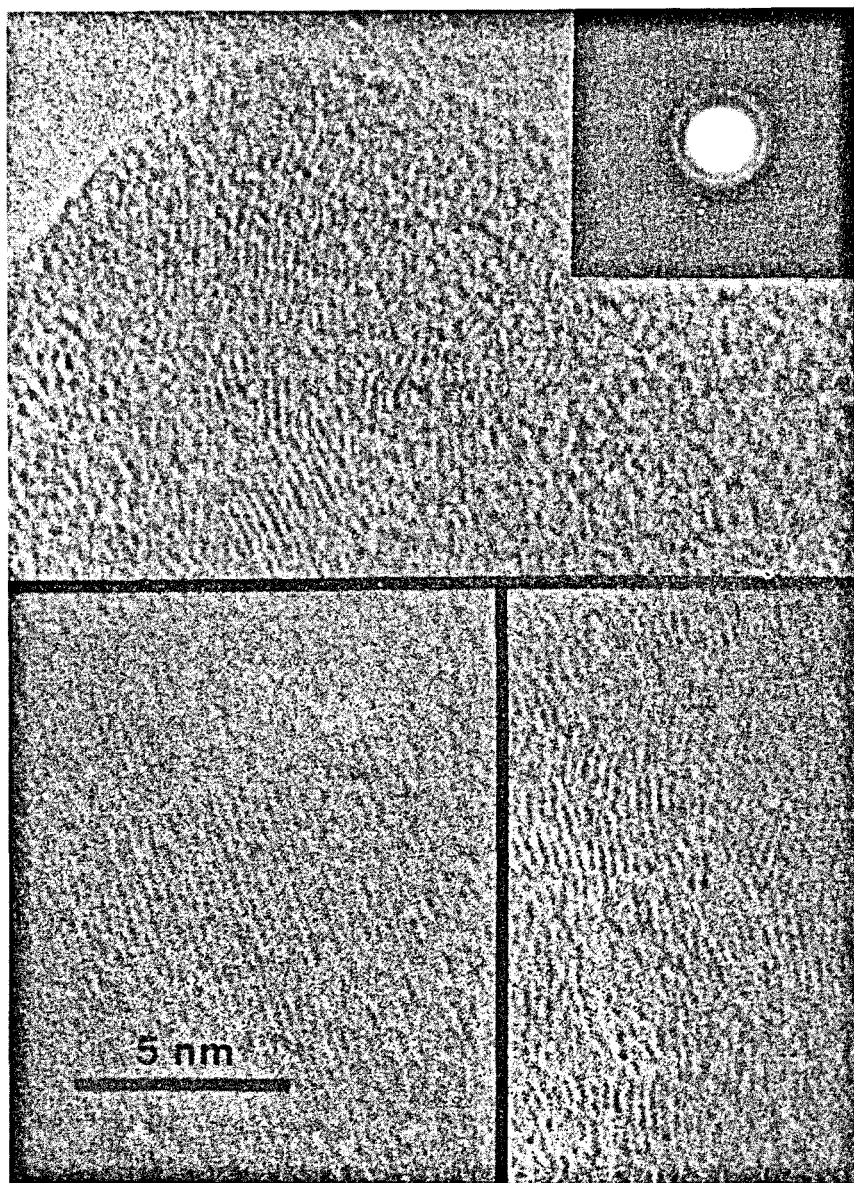


Fig.3 - TEM images of nanocrystalline GaN particles and electron diffraction ring pattern.

domains in the lower nanometer range, i.e. below 10 nm, with a significant fraction in the 5-7 nm region. Smaller nanocrystallites were observed for the solid contained in the MeOH solution, with diameters less than 5 nm mostly in the 3 to 4 nm regime. The observed lattice fringes were randomly measured for several crystalline domains in the images and gave the reproducible spacing 2.6 Å. This corresponds well with the spacing of the (0002) planes of hexagonal GaN (2.59 Å). In order to unambiguously identify the observed crystalline phase, the selected area electron diffraction patterns were obtained. For the bulk solid, the diffraction pattern consisted of diffuse rings with numerous spots superimposed onto the rings. On the other hand, for the solid from the colloidal MeOH solution, mostly diffuse rings were observed but in a few cases sparse spots were superimposed exactly on the rings. The spots resulted from the diffraction from large crystallites while the diffuse rings were attributed to a crystal shape effect for the smallest nanocrystalline particles [21]. All the strong, well visible and weak intensity rings were unambiguously indexed as hexagonal GaN in both samples.

In addition to the formation of GaN, a significant quantity of elemental Ga was formed in these systems. This phenomenon was thought to result from inherent competition between the metathetical nitriding and the redox chemistry [5,6]. A second contaminant in the system was oxygen. The likely source of most of the oxygen was a strong ether adsorption by the products occurring during the reaction itself if carried out in diglyme and/or during Et₂O washings. The presence of oxygen in the product was directly confirmed by XPS spectroscopy that indicated Ga-O by-products. However, the product was exposed to air during XPS sample preparation and this could account for at least part of the oxygen content. The XPS study showed also the absence of bromine and lithium within the detection limits of the method. It should be noted that the formation of a surface layer of the native oxide on GaN nanoparticles could lead to realization of electronic passivation, which appears to be of utmost importance for nonlinear optical properties of quantum dots [12a].

The reactions between InBr₃ and Li₃N were highly solvent dependent and sluggish. In refluxing xylene/diglyme they yielded chunks of metallic indium and a brown solid. The pyrolysis of this solid at 250 °C gave a product for which the XRD spectrum contained diffractions that were satisfactorily assigned to elemental In and In₂O₃. On the other hand, the reaction in refluxing xylene and subsequent pyrolysis of the raw solid at 300 °C afforded a material for which the XRD diffractions could fully be assigned to indium(I) bromide, InBr, and elemental In. The XPS study of the heated product confirmed significant quantities of bromine and no detectable

amounts of lithium and, thus, supported the indium(I) bromide. A further analysis of the XPS data was consistent with the presence of In_2O_3 , a small quantity of elemental In, and some $=C=O$ bearing species. This last piece of data provided arguments for the strong ether adsorption/ether cleavage occurring in this system, which apparently contributed also to the formation of In_2O_3 .

Acknowledgement. This work was supported by the Air Force Office of Scientific Research.

REFERENCES

- [1] (a) H. Morkoç, S. Strite, G.B. Gao, M.E. Lin, B. Sverdlov, M. Burns, *J.Appl.Phys.*, 1994, **76**(3), p.1363. (b) S. Strite, M.E. Lin, H. Morkoç, *Thin Solids Films*, 1993, **231**, p.197. (c) S.Strite, H. Morkoç, *J.Vac.Sci.Technol.*, 1992, **B 10**(4), p.1237.
- [2] K. Osamura, S. Naka, Y. Murakami, *J.Appl.Phys.*, 1975, **46**, p.3422.
- [3] (a) D.A. Neumayer, J.G. Ekerdt, *Chem.Mat.*, 1996, **8**, p.9. (b) B.P. Keller, S. Keller, D. Kopolnek, W.-N. Jiang, Y.-F. Wu, H. Masui, X. Wu, B. Heying, J.S. Speck, U.K. Mishra, S.P. Denbaars, *J.Electronic Mater.*, 1995, **24**(11), p.1707. (c) R. Niebuhr, K. Bachem, K. Dombrowski, M. Maier, W. Pletschen, U. Kaufmann, *J.Electronic Mater.*, 1995, **24**(11), p.1531. (d) S.E. Hooper, C.T. Foxon, T.S. Cheng, L.C. Jenkins, D.E. Lacklison, J.W. Orton, T. Bestwick, A. Kean, M. Dawson, G. Duggan, *J.Cryst.Growth*, 1995, **155**, p.157. (e) V. Lakhotia, D.A. Neumayer, A.H. Cowley, R.A. Jones, J.G. Ekerdt, *Chem.Mat.*, 1995, **7**, p.546. (f) M.J. Almond, C.E. Jenkins, D.A. Rice, *J.Organomet.Chem.*, 1993, **443**, p.137.
- [4] (a) J.-W. Hwang, J.P. Campbell, J. Kozubowski, S.A. Hanson, J.F. Evans, W.L. Gladfelter, *Chem.Mat.*, 1995, **7**, p.517. (b) A.P. Purdy, *Inorg.Chem.*, 1994, **33**, p.282. (c) S.T. Barry, D.S. Richeson, *Chem.Mat.*, 1994, **6**, p.2220. (d) R.C. Schoonmaker, A. Buhl, J. Lemley, *J.Phys.Chem.*, 1965, **69**, p.3455. (e) T. Renner, *Z.Anorg.Allg.Chem.*, 1959, **298**, p.22. (f) R. Juza, H. Hanh, *Z.Anorg.Allgem.Chem.*, 1938, **239**, p.282.
- [5] (a) E.G. Gillan, R.B. Kaner, *Chem. Mat.*, 1996, **8**, p.333. (b) R.E. Treece, E.G. Gillan, R.B. Kaner, *Comments Inorg.Chem.*, 1995, **16**(6), p.313. (c) L. Rao, R.B. Kaner, *Inorg.Chem.*, 1994, **33**, p.3210. (d) E. Ponthieu, L. Rao, L. Gengembre, J. Grimblot, R.B. Kaner, *Sol.St.Ionics*, 1993, **63-65**, p.116. (e) R.E. Treece, G.S. Macala, L. Rao, D. Franke, H. Eckert, R.B. Kaner, *Inorg.Chem.*, 1993, **32**, p.2745. (f) R.E. Treece, G.S. Macala, R.B. Kaner, *Chem.Mat.*, 1992, **4**, p.9. (g) R.E. Treece, E.G. Gillan, R.M. Jacobinas, J.B. Wiley, R.B. Kaner, *Mat.Res.Soc.Symp.Proc.*, 1992, **271**, p.169.
- [6] (a) J.C. Fitzmaurice, I.P. Parkin, A.T. Rowley, *J.Mater.Chem.*, 1994, **4**(2), p. 285. (b) A.L. Hector, I.P. Parkin, *J.Mater.Chem.*, 1994, **4**(2), p.279. (c) A.T. Rowley, I.P. Parkin, *J.Mater.Chem.*, 1993, **3**(7), p. 689. (d) J.C. Fitzmaurice, A.L. Hector, I.P. Parkin, *J.Chem.Soc.Dalton Trans.*, 1993, p.2435. (e) A. Hector, I.P. Parkin, *Chem.Soc.Dalton Trans.*, 1993, p.1095. (f) J.C. Fitzmaurice, A. Hector, I.P. Parkin, *Polyhedron*, 1993, **12**(11), p.1295.
- [7] I.P. Parkin, A.T. Rowley, *J.Mater.Chem.*, 1995, **5**(6), p.909.
- [8] A.L. Hector, I.P. Parkin, *Polyhedron*, 1995, **14**(7), p.913.

- [9] (a) S.S. Kher, R.L. Wells, *Chem.Mat.*, 1994, **6**, p.2056. (b) S.S. Kher, R.L. Wells, *Mat.Res.Soc.Symp.Proc.*, 1994, **351**, p.293. (c) S.S. Kher, R.L. Wells, *U.S. Patent No. 5,474,591*, 1995. (d) C.R.S. Hagan, S.S. Kher, L.I. Halaoui, R.L. Wells, L.A. Coury, *Anal.Chem.*, 1995, **67**, p.528. (e) L.I. Halaoui, S.S. Kher, M.S. Lube, S.R. Aubuchon, C.R.S. Hagan, R.L. Wells, L.A. Coury, *ACS Symposium Ser.*, in press. (f) S.S. Kher, R.L. Wells, *Nanostructured Materials*, in press.
- [10] S. Böck, H. Nöth, A. Wietelmann, *Z.Naturforsch.*, 1990, **45b**, p.979. (b) H. Nöth, R. Rurländer, P. Wofgardt, *Z.Naturforsch.*, 1981, **37b**, p.29.
- [11] (a) S.R. Aubuchon, A.T. McPhail, R.T. Wells, J.A. Giambra, J.R. Bowser, *Chem.Mat.*, 1994, **6**, p.82. (b) R.L. Wells, S.R. Aubuchon, S.S. Kher, M.S. Lube, P.S. White, *Chem. Mat.*, 1995, **7**, p.793.
- [12] (a) A.P. Alivisatos, *Science*, 1996, **271**, p.933. (b) L.J. Brus, *J.Chem.Phys.*, 1994, **80(9)**, p.4403. (c) M.L. Steigerwald, L.J. Brus, *Acc.Chem.Res.*, 1990, **23**, p.183. (d) A.P. Alivisatos, A.N. Goldstein, *U.S. Patent No. 5,262,357*, November 16, 1993. (e) M.A. Reed, *Scientific American*, January 1993, p.118.
- [13] (a) B.K. Laurich, D.C. Smith, M.D. Healy, *Mat.Res.Soc.Symp.Proc.*, 1994, **351**, p.49. (b) O.T. Micic, J.R. Sprague, C.J. Curtis, K.M. Jones, J.L. Machol, A.J. Nozik, H. Giessen, B. Fluegel, G. Mohs, N. Peyghambarian, *J.Phys.Chem.*, 1995, **99**, p.7754. (c) W.E. Buhro, *Polyhedron*, 1994, **13(8)**, p.1131. (d) M.A. Olschavsky, A.N. Goldstein, A.P. Alivisatos, *J.Am.Chem.Soc.*, 1990, **112**, p.9438. (e) E.K. Byrne, L. Parkanyı, K.H. Theopold, *Science*, 1988, **241**, p.332. (f) A.A. Guzelian, J.E.B. Katari, A.V. Kadavanich, U. Banin, K. Haban, E. Juban, A.P. Alivisatos, R.H. Wolters, C.C. Arnold, J.R. Heath, *J.Phys.Chem.*, 1996, **100**, p.7212.
- [14] D.F. Shriver, M.A. Drezdson, *The Manipulation of Air Sensitive Compounds*; Wiley-Interscience, New York, 1986.
- [15] (a) J.W. Trainor, K. Rose, *J.Electronic Mater.*, 1974, **3(4)**, p.821. (b) J.B. MacChesney, P.M. Bridenbaugh, P.B. O'Connor, *Mat.Res.Bull.*, 1970, **5**, p.783.
- [16] (a) B.R. Natarajan, A.H. Eltoukhy, J.E. Greene, T.L. Barr, *Thin Solid Films*, 1980, **69**, p.201 (Part I), p.217 (Part II). (b) J. Kouvetakis, D.B. Beach, *Chem.Mat.*, 1989, **1**, p.476.
- [17] (a) F.M. Elms, M.G. Gardiner, G.A. Koutsantonis, C.L. Raston, *J.Organomet.Chem.*, 1993, **449**, p.45. (b) F.R. Bennett, F.M. Elms, M.G. Gardiner, G.A. Koutsantonis, C.L. Raston, N.K. Roberts, *Organometallics*, 1992, **11**, p.1457. (c) K.J.L. Paciorek, J.H. Nakahara, L.A. Hoferkamp, C. George, J.L. Flippen-Anderson, R. Gilardi, W.R. Schmidt, *Chem.Mat.*, 1991, **3**, p.82. (d) J.F. Janik, E.N. Duesler, R.T. Paine, *Inorg.Chem.*, 1987, **26**, p.4341. (e) C.K. Narula, D.A. Lindquist, M.M. Fan, T.T. Borek, E.N. Duesler, A.K. Datye, R. Schaeffer, R.T. Paine, *Chem.Mat.*, 1990, **2**, p.377.
- [18] (a) H. Uchida, C.J. Curtis, A.J. Nozik, *J.Phys.Chem.*, 1991, **95**, p.5382. (b) L. Butler, G. Redmond, D. Fitzmaurice, *J.Phys.Chem.*, 1993, **97**, p.10750.
- [19] (a) V.L. Colvin, A.N. Goldstein, A.P. Alivisatos, *J.Am.Chem.Soc.*, 1992, **114**, p.5221. (b) C.H. Fischer, A. Henglein, *J.Phys.Chem.*, 1989, **93**, p.5578. (c) S. Yanagida, T. Ogata, A. Shindo, H. Hosokawa, H. Mori, T. Sakata, Y. Wada, *Bull.Chem.Soc.Jpn.*, 1995, **68**, p.752. (d) R.A. Hobson, P. Mulvaney, F. Grieser, *J.Chem.Soc., Chem. Commun.*, 1994, p.823. (e) H. Noglik, W.J. Pietro, *Chem.Mat.*, 1995, **7**, p.1336.
- [20] M.G. Bawendi, A.R. Kortan, M.L. Steigerwald, L.E. Brus, *J.Chem.Phys.*, 1989, **91**, p.7282.
- [21] (a) M. Brust, J. Fink, D. Bethell, D.J. Schiffrin, C. Kiely, *J.Chem.Soc., Chem. Commun.*, 1995, p.1655. (b) T.J. Cumberbatch, A. Putnis, *Mat.Res.Soc.Symp.Proc.*, 1990, **164**, p.129.